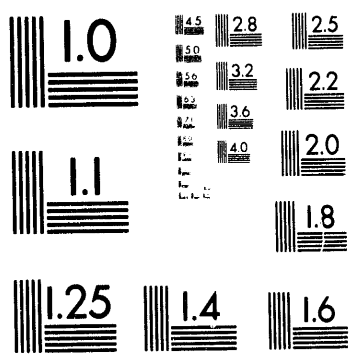
1.0
4.5
2.8
2.5
5.0
3.2
2.2
5.6
3.6
2.0
4.0
1.1
1.8
1.25
1.4
1.6

IS-M 775
Conf-940229--1

FRACTURE BEHAVIOR OF 20%Nb PARTICULATE REINFORCED ALUMINA COMPOSITE

S. Lane, S.B. Biner and O. Buck

Ames Laboratory
Iowa State University
Ames, Iowa 50011 U.S.A

Abstract

The composites consist of alumina matrix with 0.05wt% MgO and 20vol% Nb with an average particle size of 30 and 100 microns produced by dry mixing and sintering to near their theoretical densities. Fracture toughness tests were carried out in three point bending on chevron notched samples. The results indicate that R-curve of the composites exhibited more than a 300% increase in the crack growth resistance compared to the crack growth resistance of the alumina produced with the identical procedure. The crack growth resistance curve of the composites increased with increasing Nb particle size. The metallographic investigation indicated that the failure of the Nb particles in the crack path ranges from full interface separation without any significant deformation of Nb particles to cleavage failure without any evidence of interface separation.

Introduction

There is an ever increasing interest in developing low density advanced material systems for service temperatures up to 1400°C. These materials should have good fracture toughness at low and intermediate temperatures combined with good creep resistance at elevated temperatures. Recent experimental studies have shown that brittle materials such as intermetallics and ceramics can be substantially toughened by the incorporation of ductile reinforcements (1-8). The primary mechanism responsible for the enhanced toughness appears to be bridging of crack faces by intact ligaments of the ductile phase behind the advancing crack tip. Other effects such as crack deflection and crack trapping by ductile phase may also contribute. It is also observed that the toughening contribution of a ductile phase can be further increased by modification of the interface characteristics to promote debonding between the reinforcement and the matrix (4). The analyses available on the toughening behavior due to the ductile reinforcement are, in general, based on the assumption of small-scale bridging of an infinite crack in infinite geometry(9-13). However, the bridging zone is often a significant fraction of crack length. Moreover, in most modelling studies the influence of the ductile phase is directly related to its volume fraction and its geometrical parameters such size, shape, orientation and distribution are not implicitly included in the analyses.

In this study, the fracture behavior of alumina containing 20 vol% Nb particles with two different mean size distributions is experimentally investigated and compared with the failure characteristics of alumina. The observed fracture behavior is also discussed within the framework of the most recent models of ductile reinforcement toughening.

Experimental Studies and Results

The alumina powder used in the preparation of the samples had a mean particle diameter of 0.36 microns and contained 0.05wt% MgO as a sintering aid. Two different mean size distributions of irregularly shaped Nb powders, approximately 30 and 100 microns, were used to produce 20vol% Nb reinforced composites. A relatively homogenous mixing of the two powders was achieved by ball-milling for five hours in an alumina media. The mix was cold isostatically (CIP) pressed at 200 MPa for about 30 seconds to obtain approximately 50% dense green bodies. For composites and the matrix, greater densities than 99% of theoretical were achieved by [illegible] sintering at 1650°C for four hours. The final forms after [illegible]ing were rods approximately 50mm in length and 40mm in diameter. These rods were subsequently machined into fracture [illegible]ness testing samples. The resulting microstruc[illegible] the two composites are shown in Fig. 1. As can be see[illegible] distribution of the Nb phase was [illegible] uniform for both [illegible]izes. A [illegible] micrograph of the [illegible] near the interface [illegible] the Nb particle and the alumina matrix is shown in Fig. 1c. [illegible]EM and x-ray analyses did not indicate presence of any reac[illegible] phase between the Nb particles and the matrix. Additionally, no interface separation between the two phases during the processing was noticeable. Some dislocation substructure was observed in the Nb particles in spite of extremely close thermal expansion coefficients between the two phases (for Nb 8.4×10^{-6} and for alumina 8.5×10^{-6} mm/mm/°C).

Fracture toughness values were determined in three point bend using a span length of 35mm on the chevron notched samples having a thickness of 5mm and a width of 10mm. In the samples the tip of the chevron notch is located 3mm below the top surface and the chevron angle was 45 degrees. The advantages of using chevron notched samples in the assessment of fracture toughness of the brittle materials are well documented. A sharp crack is produced during the loading, therefore, neither fatigue precracking nor the measurement of the crack length is required and the resulting fracture toughness is estimated from:

$$K_{IC} = \frac{P_{max} A}{B\sqrt{W}} \qquad (1)$$

where P_{max} is the maximum load measured during the test, A is a constant, B is the thickness and W is the width of the sample. For this test geometry, the crack resistance curves can also be estimated with a procedure based on the J-integral concept as described in ref.(14). In order to determine the value of constant A in eq. (1). specific to our chevron notch geometry and also for the estimation of the crack lengths from the unloading compliance values, the compliance analysis was carried out by the procedure outlined in ref.(15). The tests were carried out on 20 KN screw driven Instron testing machine with a loading rate of 0.01 mm/min. The observed load versus load-line-displacement (LLD) curves are shown in Fig. 2 for the alumina and the Nb reinforced composites. The unloading-reloading cycles which were used to determine the crack lengths can be seen in the figure. After the maximum load, large and unstable crack extension were observed in the alumina samples. In the case of the Nb reinforced composites the crack extensions were stable and even after large crack extensions the unloading-reloading cycles were successfully completed. The maximum load values for the composites were not significantly higher than the ones observed for the alumina; however, the composite with larger Nb particles gave the highest maximum load levels. Substantial increases in the total energy required for complete failure of the composites can be seen in Fig. 2. The resulting R-curves for the alumina matrix and composites with the procedure described in ref.(14) are summarized in Fig. 3. From these results, the steady-state fracture toughness value for the alumina is determined to be 4.2 MN $m^{-3/2}$ which is very close to the reported value(16) for alumina with a similar grain size. On the other hand, R-curves were still rising at the conclusion of the tests for both composites, thus indicating that steady state fracture was not achieved. Nonetheless, when a comparison is made for final crack lengths, a net increase of about 300% in the toughness values of the large Nb containing composite can be seen.

The role of the reinforcement and the size effect was elucidated with examination of the fracture paths on the interrupted tests and with fractographic studies of the fracture surfaces. These samples were in standard three point bending configuration and polished before the introduction of the macroscopic cracks. An example of the interaction between the Nb particle and the crack path is given in Fig. 4. The figure indicates that there is almost no evidence of interface separation or extensive deformation of the Nb particle. On the other hand, Fig. 5 shows a Nb particle at the crack path and the failure is completely due to the interface separation and particle pull-out. The evidence of large scale interface separation combined with the partial cleavage failure of the Nb particle is shown in Fig. 6. The impression of the neighboring alumina grains decorates the Nb particles. Interface separation to a lesser extent accompanied by complete cleavage failure of the Nb particle can be seen in Fig. 7. The failure of the matrix material betwe n the Nb particles was identical to that observed in alumina alone and composed of multiple cracking, crack branching and grain pull-out.

Discussion

In the modelling of the fracture toughness of the composites due to crack bridging by the ductile particles, the stress intensity factor due to the applied stress is usually described as

$$K^{applied} = K_{bridge} + K_{tip} \qquad (2)$$

At any given applied stress, the magnitude of K_{bridge} is calculated from the work of fracture of one ligament taking into account the volume fraction, V_f of the ductile reinforcement. The work of fracture, per unit area of the crack face is given as(2)

$$\Delta G = V_f \int_0^{u^*} \sigma(u)\, du \qquad (3)$$

where $\sigma(u)$ is the nominal stress required to stretch a ligament by u and u^* is its failure stretch. When $\sigma(u)$ is constant from u to u^* (i.e., if there is no significant work hardening in the ductile particles) the result is:

$$\Delta G = V_f \sigma_{max} u^* \qquad (4)$$

and

$$K^{applied} = K_{tip} + [\frac{E}{(1-\nu)^2} \Delta G]^{1/2} \qquad (5)$$

The same result is obtained by considering the reduction in $K^{applied}$ caused by a distribution of $\sigma(x)$ of closing stress, acting between the crack tip and a distance L (the steady-state bridging length) behind the crack tip. This relation is given as (17)

$$K_{bridge} = (\frac{2}{\pi})^{1/2} \; V_f \int \frac{\sigma(x)}{\sqrt{x}}\, dx \qquad (6)$$

For a constant bridging stress , $\sigma(x)=\sigma_{max}$ from $x=0$ to $x=L$,

$$K_{bridge} = \left(\frac{8L}{\pi}\right)^{1/2} V_f \sigma_{max} \tag{7}$$

As can be seen in both approaches the quantitative determination of the bridging contribution requires an estimation of the failure stress of the particles. Usually this is taken as the bulk yield strength of the non-work hardening ductile reinforcing phase. By using the experimentally measured fracture toughness values and by taking the σ_{max} for Nb particles as 300 MPa(3), the estimated crack bridging zone for large Nb containing composite is found to be about 8mm which scales with the experiments (i.e., the lack of plateau in the reinforced composites is due to smaller crack length than the estimated bridging lengths). However, caution should be exercised in the quantitative estimation of the fracture toughness values resulting from crack bridging. As can be seen from the above analyses, the contribution of the ductile phase is included in terms of only volume fraction and its geometrical parameters such as size, shape, orientation, distribution and interfacial behavior are not implicitly considered (except in ref(10,11)). As demonstrated in this study, for a given volume fraction, the size of the reinforcing phase plays a significant role in the toughening behavior. Also, a recent numerical analysis(18) indicates that a considerable amount of hydrostatic stress build-up occurs in the ductile particles as result of constraint induced by the matrix which may cause failure of the particles before any significant deformation such as is seen in Fig. 4. In this case the value σ_{max} could be several times the yield strength of the ductile reinforcing phase. In the light of these analyses we expect a larger increase in the steady state fracture toughness value of the Nb reinforced composite than the ones observed in this study.

Conclusions

In this study, the fracture behavior of alumina containing 20vol% Nb particles with two different mean size distributions is experimentally investigated. The results indicate that:

1. The R-curves of the composites exhibited more than a 300% increase in the crack growth resistance over that of the alumina produced with the identical procedure.
2. The crack growth resistance curve of the composite increases with increasing Nb particle size.
3. The failure of the Nb particles in the crack path ranged from full interface separation with [illegible] significant deformation of Nb particles to cleavage [illegible] without evidence of interface separation.

Acknowledgement

This work was performed for the United Stat[illegible]tment of Energy by Iowa State University under contract [illegible] Eng-82. This research was supported by the Director of [illegible] Research, Office of Basic Energy Sciences.

References

1. C. K. Elliot, G. R. Ode[illegible] G. E. Lucas and J. W. Sheckard, <u>MRS Proc.</u>, 120 (1988), 95.

2. M. F. Ashby, F. J. Blunt and M. Bannister, <u>Acta Metall. Mater.</u>, 37 (1989), 1847.

3. P. Mataga, <u>Acta Metall. Mater.</u>, 37 (1989), 3349.
4. T. C. Lu, A. G. Evans, R. J. Hecht and R. Mehrabian, <u>Acta Metall. Mater.</u>, 39 (1991), 1853.

5. B. D. Flinn, M. Ruhle and A. G. Evans, <u>Acta Metall.</u>, 37 (1989), 3001.

6. M. Bannister, H. Shercliff, B. Bao, F. Zuk and M. F. Ashby, <u>Acta Metall.</u>, 40 (1992), 1995.

7. L. S. Sigl, A. G. Evans, P. A. Mataga, R. M. McMeeking and B. J. Dalglesh, <u>Acta Metall.</u>, 36 (1988), 945.

8. T. S. Oh, J. Rodel, R. M. Cannon and R. O. Ritchie, <u>Acta Metall.</u>, 36 (1988), 2083.

9. M. A. Prystupa and T. H. Courtney, <u>Metall. Trans. A.</u>, 13 (1982), 873.

10. B. Budinsky, J. C. Amizigo and A. G. Evans, <u>J. Mech. Phy. Solids</u>, 36 (1988), 167.

11. F. Erdogan and P. F. Joseph, <u>J. Am. Ceram. Soc.</u>, 72 (1989), 262.

12. K. S. Ravichandran, <u>Acta Metall. Mater.</u>, 40 (1992), 1009.

13. M. Bannister, H. Sheriff, G. Bao, F. Zok and M. F. Ashby, <u>Acta Metall. Mater.</u>, 40(1992), 1531.

14. S. B. Biner, A. Samkary and N. A. Ibrahim "Determination of J_{Ic} From Chevron Notched Three Point Bending Specimens in Elastic-Plastic Range," <u>The Mechanism of Fracture</u>, ed. V.S. Goel (ASM, Metals Park Ohio, 1986), 127.

15. S. B. Biner, J. T. Barnby and D. W. J. Elwell, <u>Int. J. Fract.</u>, 26 (1984), 3.

16. G. Vekins, M. F. Ashby [illegible] P. W. R. Beaumont, <u>Acta Metall. Mater.</u>, 38 (1990), 1151.

17. H. Tada, P. C. Paris [illegible] G. R. Irwin, <u>Stress Analysis Handbook</u>, (Del. Res. Corp., [illegible], MO, 1985).

18. S. B. Biner, "A Nume[illegible]lysis [illegible] Fracture and High Temperature Creep Characte[illegible] of Brittle Matrix Composites With Discontinuous Ductile [illegible]forcements," Submitted to <u>Mat. Sci. Eng.</u>

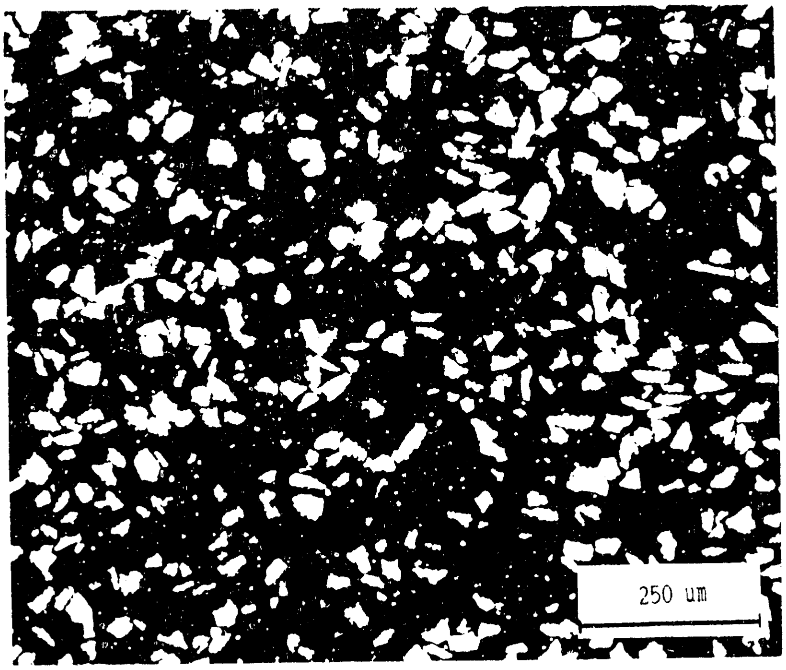

Fig. 1a Microstructure of alumina reinforced with 30 micron Nb.

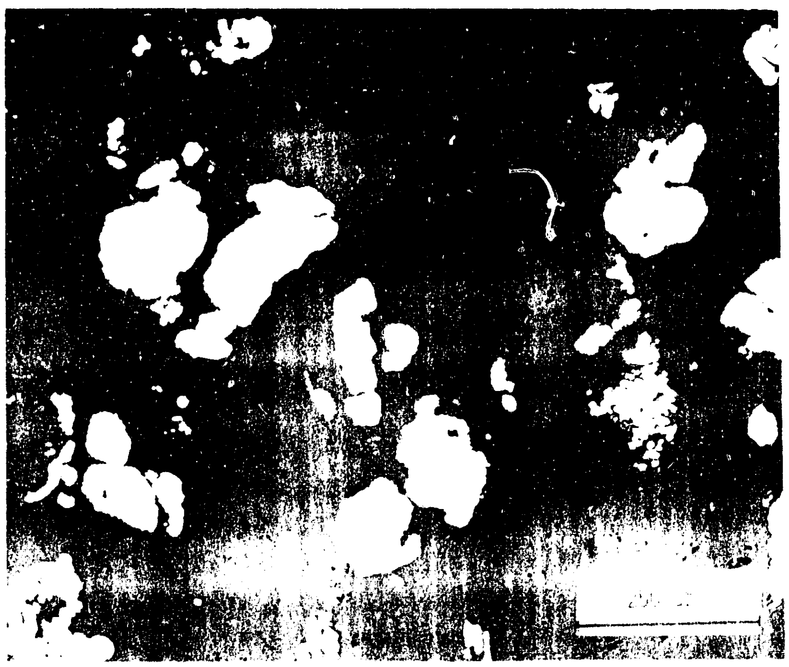

Fig. 1b Microstructure of alumina reinforced with 100 micron Nb.

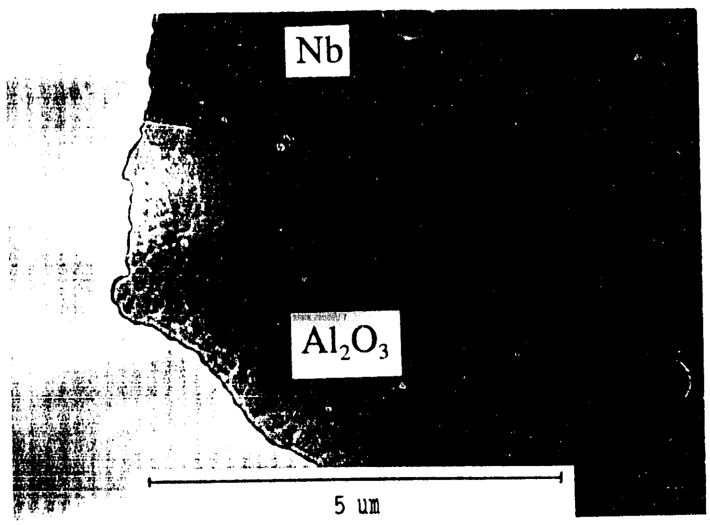

Fig. 1c TEM micrograph of typical Nb/alumina interface.

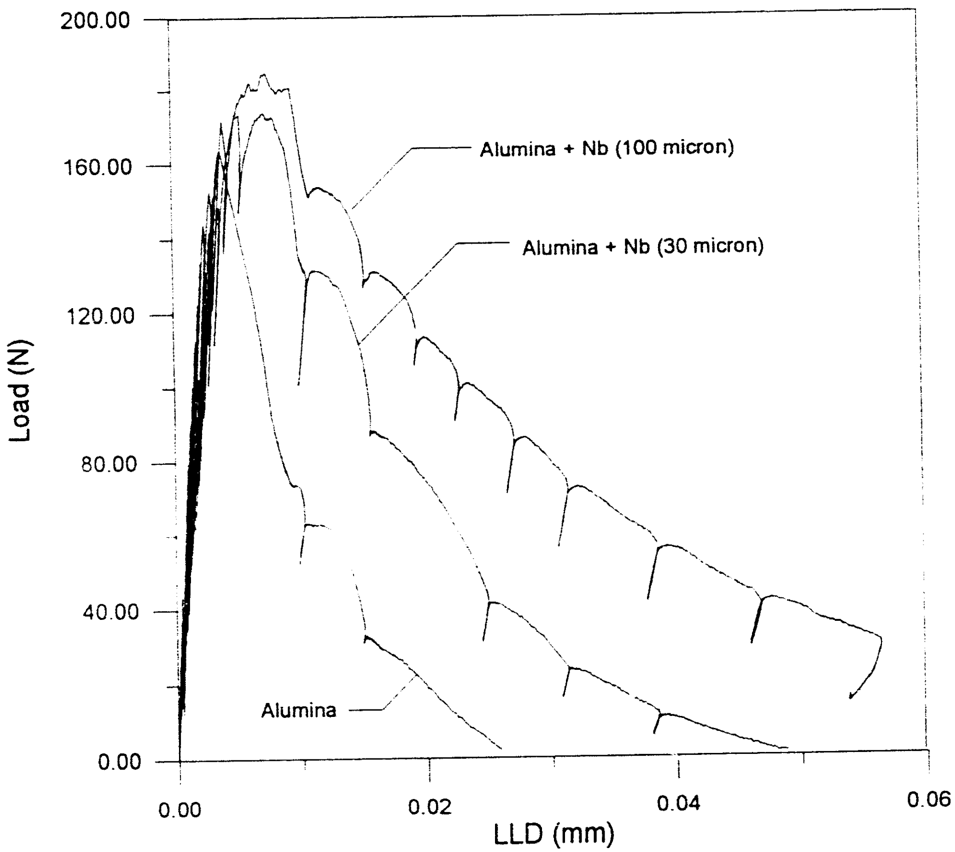

Fig. 2 Load versus load-line-displacement (LLD) curves for alumina and Nb reinforced composites.

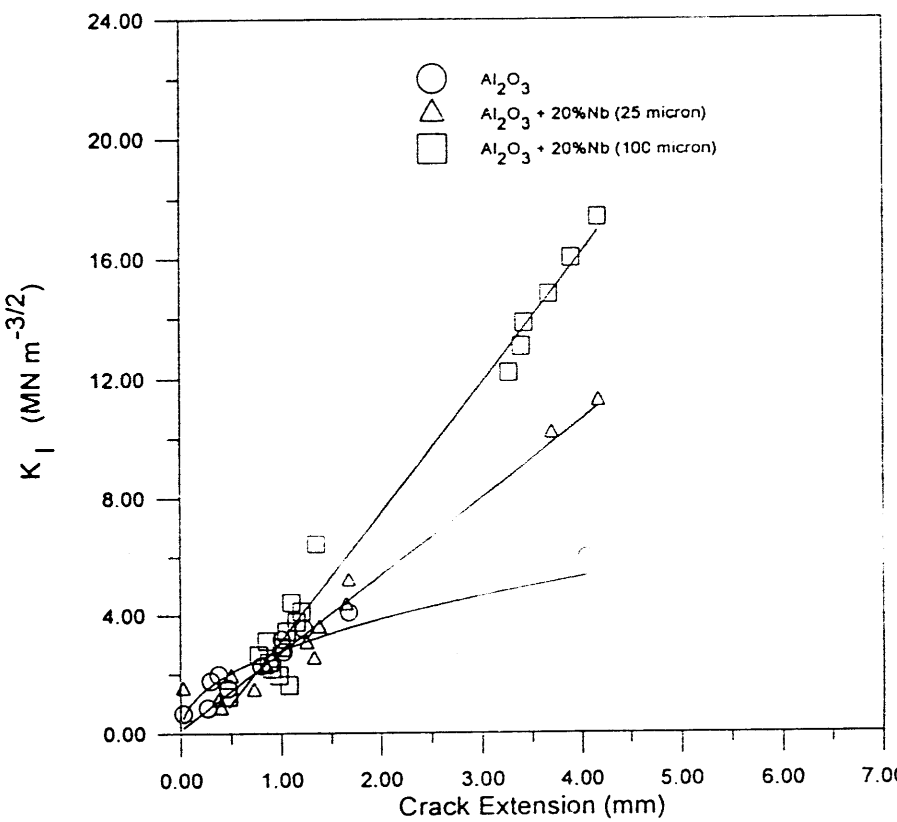

Fig. 3 R-curves for alumina and Nb reinforced composites.

11 6 S. Lane

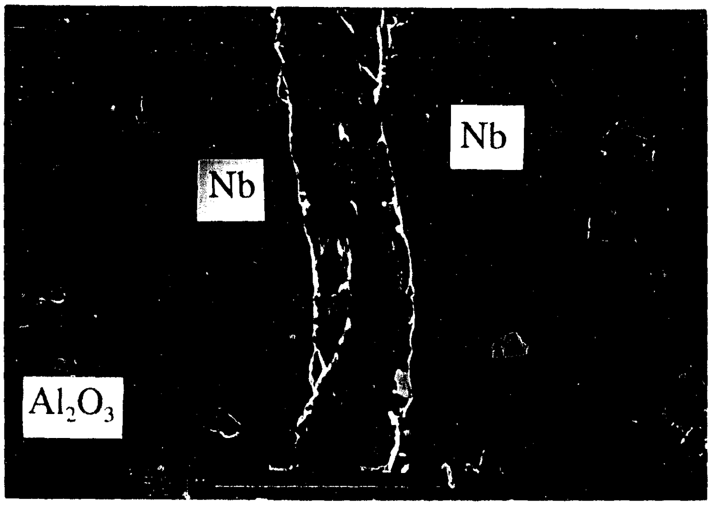

Fig. 4 Interaction of crack and Nb particle resulting in particle fracture without separation from the matrix.

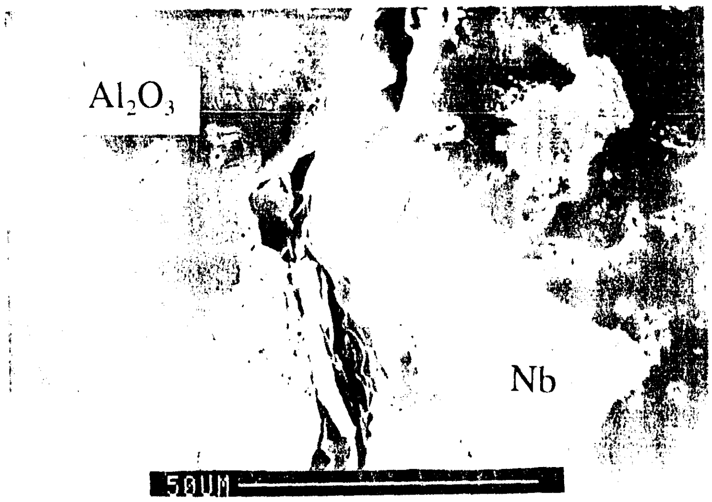

Fig. 5 Crack particle interaction resulting in interfacial separation and particle pullout.

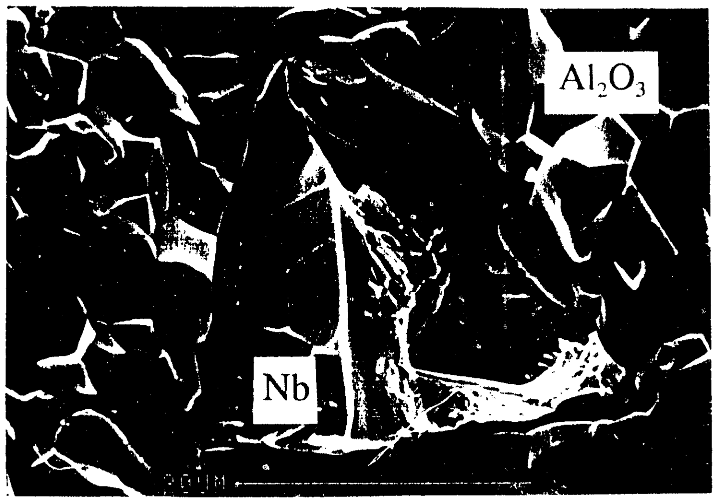

Fig. 6 Interaction of crack and Nb reinforcement resulting in interface separation and partial cleavage.

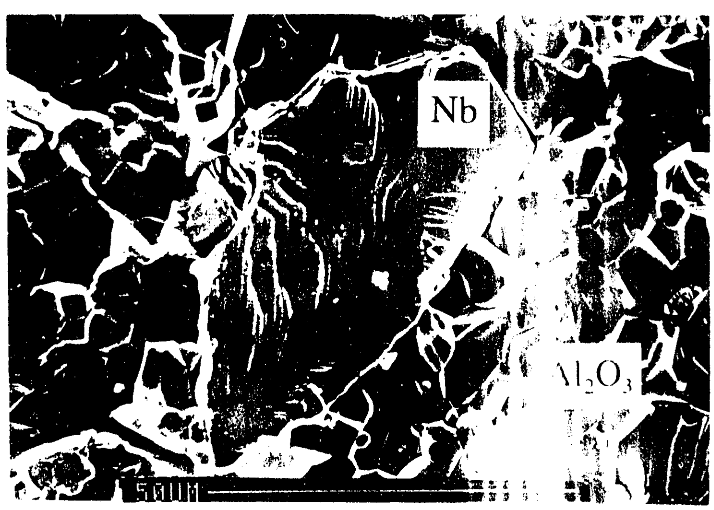

Fig. 7 Crack/particle interaction resulting in slight interface separation and complete cleavage of Nb.

DATE
FILMED
1 / 6 / 94

END